



ELSEVIER

Journal of Chromatography A, 943 (2001) 15–31

JOURNAL OF
CHROMATOGRAPHY A

www.elsevier.com/locate/chroma

Behavior of packing materials in axially compressed chromatographic columns

Djamel E. Cherrak^{a,b,1}, Majed Al-Bokari^{a,b}, Eric C. Drumm^c, Georges Guiochon^{a,b,*}

^aDepartment of Chemistry, University of Tennessee, Knoxville, TN 37996-1600, USA

^bDivision of Chemical and Analytical Sciences, Oak Ridge National Laboratory, Oak Ridge, TN 37831-6120, USA

^cDepartment of Civil and Environmental Engineering, University of Tennessee, Knoxville, TN 37996-2010, USA

Received 13 August 2001; received in revised form 22 October 2001; accepted 23 October 2001

Abstract

The behavior of a packing material (Luna C₁₈ from Phenomenex, Torrance, CA, USA) was studied during the consolidation of a column bed under axial compression stress. The kinetics of this consolidation, the permeability and efficiency of the columns obtained, and the reproducibility of these column properties were measured under different conditions. The consolidation process and the column properties are considerably affected by the friction between the packing material in the bed and the column wall. Clear evidence of this wall effect was demonstrated. The apparent permeability of columns consolidated under the same axial stress increases with increasing column length. The apparent modulus of elasticity of the beds increases with increasing column length. The shear resistance between the packed bed and the column wall was measured for columns of different lengths. It increases rapidly with increasing bed length. The column efficiency for thiourea (unretained) and phenyloctane (retention factor, $k' \approx 1$) was much poorer after recompression than after the first compression. It depended little on the compression stress. The effect of the column length was small. © 2002 Elsevier Science B.V. All rights reserved.

Keywords: Column packing; Axial compression; Shear stress; Wall effects; Thiourea; Phenyloctane

1. Introduction

Dynamic axially compressed (DAC) columns, packed with small or moderate size particles ($d_p = 10\text{--}30\ \mu\text{m}$), are increasingly used in preparative liquid chromatography [1]. There are now several suppliers of axial compression column skids with

column bodies between ca. 2.5 and 7.5 cm I.D. while industrial-size units incorporating columns up to 80 cm I.D. are available from at least one of these manufacturers. Lately, a newly designed dynamic axial compression packing system was introduced [2] and tested [3].

A spring apparatus maintains the packed bed under pressure and the removal of the column without disturbing the bed, so the system can be used to pack other columns. It seems that the performance of the column remains satisfactory and that dynamic compression of a properly consolidated bed is not necessary [3].

*Corresponding author. Tel.: +1-865-974-0733; Fax: +1-865-974-2667.

E-mail address: guiochon@utk.edu (G. Guiochon).

¹Present address: Labmetrix Technologies, Newport Beach, CA, USA.

The column efficiency is the most fundamental property characterizing its performance in liquid chromatography [4]. However, close behind are more mundane, yet essential properties such as the stability and the reproducibility of the column characteristics.

This last property is particularly important in the implementation of simulated moving bed (SMB) chromatography. This application requires the use of a set of columns having identical or closely similar properties (e.g. porosity, retention factor, selectivity, permeability, efficiency, etc.) for the optimization of SMB process. Fluctuations of column properties translate into a loss of production rate [5]. All the properties just listed depend on the packing density. Accordingly, the control of the packing procedure is of critical importance in the reproducible preparation of columns. The

DAC method affords the most reproducible and fastest way of packing highly efficient columns for preparative liquid chromatography. The parameters that influence the stability of the bed and the reproducibility of its performance were recently studied [6–10]. It was shown that the nature of the slurry solvent [6], the intensity of the compression stress, the rate at which this stress is applied, and the nature of the mobile phase (often different from the slurry solvent) may dramatically affect the packing density and the column efficiency [7–10]. Obviously, the best slurry solvent is a function of the nature (rigid inorganic oxide or soft polymer), the surface chemistry [6], and the geometry (regular or spherical) of the sorbent particles [11].

Cherrak and Guiochon [10] measured the friction shear-stress between a bed of Kromasil C₈ and the column wall, and demonstrated that this friction is intense. The intensity of the friction shear stress was found to increase rapidly with increasing column length and to depend strongly on the nature of the slurry solvent used to disperse the particles [10]. This phenomenon is the essential cause of what is known as the wall effect, the formation in chromatographic columns of a wall region having physical properties different from those of the core region [12]. The friction of the bed against the wall causes systematic radial and axial variations of the packing density, i.e. of the local porosity of the bed, which in turn causes a trans-column variation of the bed

permeability, hence a warping of the injected band during its migration, resulting in an apparent band broadening and a real loss of band resolution [8–10,13–17]. It also explains why the packing density and the column permeability increase significantly with increasing bed length [9,10]. This effect prevents the preparation of long columns, e.g. those of 5 cm I.D. exceeding approximately 30 cm (1 ft).

The search for the experimental packing conditions that maximize the column efficiency has attracted the most attention [10,18]. Cherrak and Guiochon [10] compared the influence of several slurry solvents on the performance of columns packed with reversed-phase Kromasil C₈ and found that the minimum height equivalent to a theoretical plate (HETP) was weakly correlated with the viscosity of the slurry solvent used in DAC for RPLC. The densest packing bed did not produce the best performance. Moscariello et al. [18] investigated the influence of the slurry concentration on the column efficiency and found a minimum of the HETP at constant flow-rate for a slurry concentration of ca. 20% (v/v).

Several other factors influence the separation in preparative chromatography, e.g. an uneven distribution of either the injected solute band at the inlet or of the collected fractions at the outlet of the column or a heterogeneous distribution of the temperature in the column [19]. Brandt et al. discussed the distribution of temperature within the bed in DAC columns, a function of the bed heterogeneity, of the nature of the packing, of the degree of band spreading in the inlet and outlet frits, and of properties of the eluent (e.g. its thermal conductivity, heat capacity, and viscosity) [14,15]. Lode et al. [13] investigated the problems associated with a homogeneous distribution of the band at the column inlet.

The use of DAC was extended to soft packing materials [20–22]. In this case, Danilov and co-workers [20,21] observed a linear decrease of the bed length with increasing axial compression stress (up to ca. 30 kPa) [20,21], and noticed that the stabilization of the bed length was very slow. The compression of the bed caused an important decrease of its porosity, due to both the consolidation of the bed and particle deformation. The authors also reported that the bed length increased very slowly when the stress was released from 30 kPa to zero and

did not return to its initial length, although no significant deformation of the spherical shape of the Sephadex gel beads was observed during bed relaxation. They also observed that 1–2% of the particles were damaged during the compression. Similar results were observed for columns packed with Bio-Gel P2 [22].

Further studies are needed in order better to understand the DAC process of column packing and to make possible the reproducible preparation of highly efficient columns.

The aim of this work is to study the kinetics of consolidation of columns, the influence of the intensity of the axial compression stress on the column length or its permeability and on its efficiency, and the influence of the bed length on the wall-friction shear-stress.

2. Experimental

2.1. Equipment

An LC-50 dynamic axial compression column skid (Prochrom, now Novasep, Nancy, France) was used to pack, prepare, and operate the columns [7]. The bed of packing material is compressed by a piston moving inside a cylinder or column body. This piston is actuated by a hydraulic jack. The column body is a stainless steel cylinder 5 cm I.D., designed to allow a maximum hydrostatic pressure of approximately 100 kg/cm². A Dynamax SD1 (Rainin, Woburn, MA, USA) pump equipped with dual pistons was used as the solvent delivery system. The maximum flow-rate is 800 ml/min and the maximum pressure 1500 p.s.i. (ca. 105 bar). The UV detector was a SpectraFocus from Thermoseparation Products, Riviera Beach, FL, USA, equipped with a preparative flow cell (optical path length, 2.8 mm) throughout all the experiments reported here. The UV signal was recorded at a wavelength of 254 nm (unless otherwise specified). A six-port electro-pneumatic switching valve was used to inject the sample. For all the experiments, the sample volume was 0.5 ml. The special top flange described earlier [9], fitted with a 30 mm extension, was used during all these experiments in order to allow the successive determination of the column characteristics and the

friction properties, with no need to disturb or move the consolidated bed.

The column inlet pressure (ΔP) was measured with an Omega pressure transducer Model PX603-2KG5V (Stamford, CT, USA). This transducer allows the measurement of pressures up to 140 bar with a response time of 1 ms. Dynamic changes of the bed length smaller than 1 cm (accuracy, 0.01 mm) were measured with an Electro-Mike displacement sensor Model PAA1555 (Reagan Controls, Charlotte, NC, USA). This sensor includes a displacement transducer and a transmitter with an analog output. Larger changes in the bed length were derived from the displacement of an index fixed to the piston, measured with a ruler (accuracy ca. 1 mm). The electrical signals of the displacement sensor, the pressure transducer, and the UV detector were collected with the data acquisition system Maxima 820, version 3.3 (Waters, Milford, MA, USA). All the data files were translated into ASCII format and downloaded to one of the computers of the University of Tennessee Computer Center for further data processing.

A 250×4.6 mm analytical column was packed in our laboratory, using the conventional slurry packing method with methanol, at a maximum pressure of 300 bar. The same packing material as for the preparative column was used. The characteristics of this column were measured with an HP1090 liquid chromatograph (Hewlett-Packard, Palo Alto, CA, USA) equipped with a ternary solvent delivery system, a diode array UV detector and a data station.

2.2. Packing material

All the columns studied were packed with Luna C₁₈, a C₁₈ bonded, silica-based packing material for RPLC (average diameter 10 μm, spherical particles) from Phenomenex (Torrance, CA, USA).

2.3. Mobile phase and chemicals

Methanol, isopropanol and methylene chloride were used as packing solvents or mobile phases in this study. Dilute solutions (concentration lower than 0.2 g/l) of thiourea or phenyloctane (Aldrich, Milwaukee, WI, USA) in the mobile phase were injected to measure the column efficiency and the hold-up

volume, hence the total column porosity. These compounds were all HPLC grade or analytical grade (Fisher Scientific, Fair Lawn, NJ, USA). All the chemicals and solvents were used without further purification.

2.4. Procedures

2.4.1. Column packing and consolidation

All chromatographic columns were packed following the procedure previously described [7–11]. The exact amount of dry packing material required was mixed with the appropriate volume of the selected solvent and turned into a thick slurry. All the columns were packed using slurries having the same concentration (i.e. ratio of the dry-packing mass to the total volume of solvent). The slurry was stirred for several minutes in an ultrasonic bath and rapidly poured into the empty column. The column was closed, and the desired axial compression stress was rapidly applied to the column. In all cases, the axial compression pressure was increased in a series of successive steps, up to the maximum pressure compatible with the integrity of the packing particles (ca. 90 bar). The bed length was recorded during each consolidation step. When the highest compression stress was reached and no further decrease of the bed length was observed, the compression stress was abruptly released (the skid design does not allow for progressive decompression of the bed). During this decompression step, the bed length was also recorded in order to measure the elastic reaction of the packed bed.

Before each experiment, the column and its frits (at the top of the piston and under the top flange, respectively, see Fig. 1) were carefully cleaned. The fine mesh grids of the frit keep the packing particles from flowing out of the column and allow a homogenous distribution of the flow pattern over the column cross-section. However, particle breakage takes place to some extent during the consolidation of packing materials under high compression stress, even for the relatively strong spherical particles used in this work.

This breakage takes place essentially where the mechanical stress is highest, in a wedge against the piston and close to the column wall. This observation is in agreement with the findings of a rheological

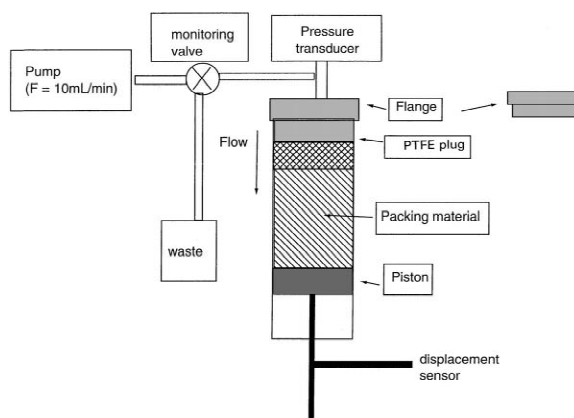


Fig. 1. Schematic design of the equipment used for the measurement of the friction shear stress. The pushing fluid fills the space between the top flange and the PTFE plug [9,10].

model of column compression [24]. Part of the fines produced by the broken particles become incrustated inside the grid at the time of particle breakage.

Others migrate along the column and may get trapped inside the outlet frit. Abrasion during handling of the packing material results also in some particle fragmentation, even with spherical particles. In all cases, these fines may cause partial obstruction of the frits (i.e. pore clogging) and an uneven flow distribution. Thus, frits must be periodically soaked in methanol and treated for 30 min in an ultrasonic bath. This procedure allows fast cleaning of the frits and nearly complete removal of the fine particles.

2.4.2. Column characteristics

For most columns packed as just described, the kinetics of consolidation of the bed, the column permeability, its porosity, and its efficiency were measured. The permeability was derived from measurements of the column inlet pressure at different mobile phase flow-rates ranging from 1 to 100 ml/min. The column efficiency was determined from the maximum of the peak of thiourea (or phenyloctane) and its width at half-height. It was measured at several flow-rates. The reduced plate height ($h = H/d_p$) was plotted vs. the reduced velocity ($v = ud_p/D_m$), with u linear velocity (mobile phase flow-rate/cross-section of the column), d_p average particle diameter, and D_m molecular diffusivity. This last coefficient was estimated for the compounds used in

this study using the classical Wilke–Chang equation [25]. The reduced velocities and the actual reduced plate heights were fitted to the van Deemter equation [26] using a nonlinear least-squares fit.

2.4.3. Friction measurements

After completion of the determination of the column characteristics, the friction between the consolidated bed and the column wall was measured following the procedure previously described [9,10], by pushing the bed out of the column (Fig. 1). During this experiment, a 25 mm long plug made of a stainless steel cylinder bolted between two solid PTFE disks, was placed on the top of the packing material, inside the column, in place of the special top flange [9,10]. This is done without moving the bed and affecting the texture or the morphology of the cake by changing the orientation of the particles. The plug prevents the flow of the mobile phase. When a pump for analytical HPLC is used to resume pumping methanol into the column at a low flow-rate, pressure rises behind this PTFE plug, tending to push the plug, the consolidated packing material, and the piston out of the column. Positioning the plug ahead of the bed prevents the solvent from reaching the packing material, mixing with it and possibly changing the bed composition or cohesion, or eroding the bed. The bed was then reconsolidated under 40 bar for about 30 min (during the last 29 of which their length remained constant), after what the stress was released, the compression piston let free to slide along the cylinder and methanol was pumped into the top of the column, at a maximum flow-rate of 10 ml/min, with a set pressure [9,10]. The set pressure was increased stepwise through an adjustable valve until the plug starts moving. The pressure of the liquid above the plug and the back displacement of the plug were recorded (Fig. 1).

3. Results and discussion

3.1. Compression kinetics and bed elasticity

Fig. 2 shows plots of the bed length versus time for a typical column packed with 200 g of Luna C₁₈, as recorded during three of the successive intermediate steps taking place in the first compression

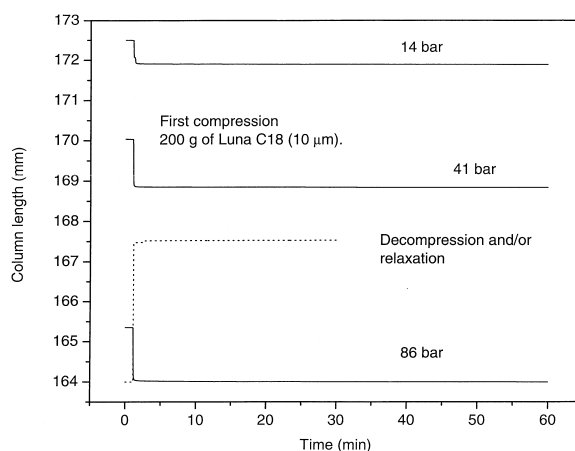


Fig. 2. Plot of the bed length vs. time (first compression). The axial compression stress applied is indicated on each solid line.

(solid lines). The compression stress was applied after recording the signal for 1 min, in order accurately to determine the rapid drop of the signal.

The application of the compression stress caused a rapid decrease of the bed length.

Because the particles of this packing material are spherical, in all cases, the bed length dropped abruptly, during the first seconds following the application of the stress, minor drops in the bed length were occasionally observed a few minutes later, and no significant variation of the bed length was observed after 60 min. Once the consolidation of the bed was completed at the applied stress, the permeability of the column was measured, and the compression stress was further increased, until eventually a maximum pressure of about 90 bar was reached. The first compression was then ended.

For all the columns studied (not all curves are shown), whatever the amount of packing material used, the bed length decreased significantly and rapidly when the stress was applied, as illustrated in Fig. 2. It should be noted, however, that monitoring of the column length over a very long time may show a slight decrease, at a rate that decreases constantly with time, yet never seems to really end. This result is in agreement with those of previous studies on the packing of spherical particles [7–11].

When the first consolidation of a bed was achieved under the maximum pressure set for this phase, the hydraulic jack actuating the piston (down or upward

movement) was abruptly released. The length of the bed bounced back rapidly when the stress was released (Fig. 2, dotted lines), because of the bed elasticity. The bed decompression, following the relaxation of the mechanical stress, caused an instantaneous increase of the interstitial void or external porosity [9,10]. However, the bed did not return to its initial bed length, ca. 173 mm, in part because of the consolidation of the bed, in part because of the wall effect [9,10]. The release of mechanical stress lets the particles, deformed by the stress, return to their initial shape. However, consolidation involves also the movement of particles by respect to each other and a reduction of the voids between them. This latter change is irreversible [23,24,27].

Once the first compression was achieved and the bed was completely relaxed, a second set of compression experiments was carried out. The axial compression stress was increased stepwise, as in the first compression, the column length being monitored likewise. All the plots (bed length vs. time) were qualitatively similar to those obtained in the first compression experience. A few of them are shown in Fig. 3. Occasionally again, a second and small drop of the bed length was observed at high stress. This was observed in the case illustrated in Fig. 3 by the drop observed after 7 min at ca. 90 bar. The second decompression following the relaxation of the mechanical stress applied to the bed caused a rapid increase of the bed length, similar to the one observed after the first decompression. This confirms

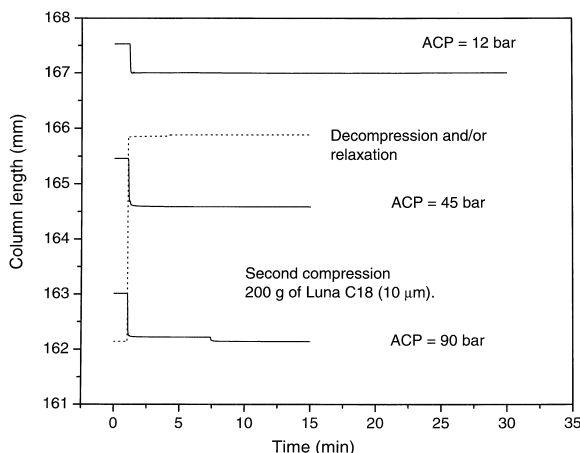


Fig. 3. Plot of the bed length vs. time (second compression).

the general behavior of axially packed columns – a fully consolidated bed expands upon release of the compression stress. Although the bed behavior under successive compressions is qualitatively similar, the numerical values vary quite significantly from one to the next, in all cases examined.

Fig. 4 illustrates the variation of the bed with the axial compression pressure for a column packed with 200 g of packing material. In all cases, the column length decreases linearly with increasing axial mechanical stress. For the first compression, the slope is significantly steeper than for the second because, during this second compression, the particles move relatively to each other to a much less significant extent than during the first one. Note, however, that, after the first decompression, the bed length did not return to its initial length (it goes to ca. 168 mm, see symbol ■ in Fig. 4) and that, after the second consolidation and compression, it remains still shorter (see symbols ▲ and ■ in Fig. 4). As we show later, this is explained by the strong friction between the particles in the bed and the friction of the bed against the column wall.

In order to better understand the process of

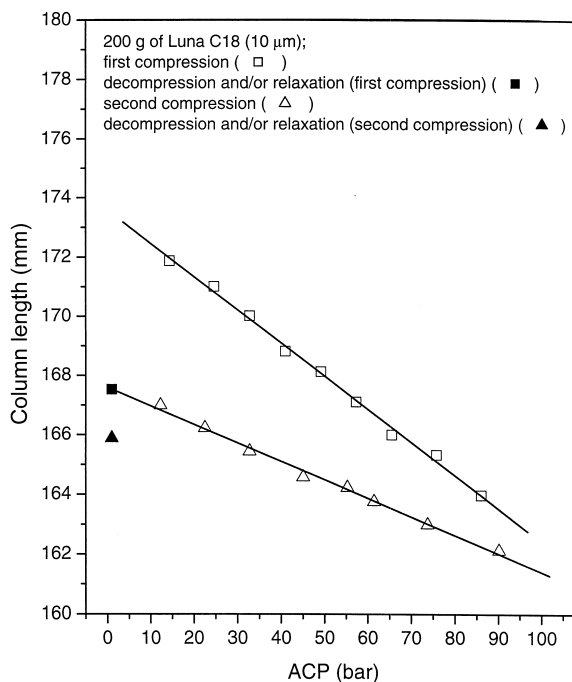


Fig. 4. Compressibility curve for a column packed with 200 g.

consolidation of beds of particulate materials such as the packing material used here, we studied the compressibility of columns packed with smaller amounts of material, namely 15, 25 and 150 g. The first two of these amounts produced very short columns, not suitable for preparative separations but useful to study because the wall effect should be less significant and the stress more uniformly distributed.

The beds prepared with these amounts were submitted to three successive stepwise compressions. First, each column was compressed up to ca. 30 bar, then, the stress was released. A second compression was carried out on the same column, this time up to a pressure of ca. 60 bar. Then, the column was decompressed for the second time, and this was followed by a third compression, to the maximum allowed by the equipment (ca. 90 bar). Finally, the stress was released after completion of this third series of compression experiments, and the bed was left free to expand a last time. Figs. 5–7 depict the variation of the bed length with the axial compression stress applied to the three columns.

It is worth noting that all three columns exhibit the same compressibility behavior (Figs. 5–7). The slopes of the plots of the bed length vs. the mechanical stress decrease from the first to the third consolidation. The extent of bed expansion associated with a decompression decreases from the first to the third successive decompression of all columns (see solid symbols in Figs. 5–7). Fig. 7 also com-

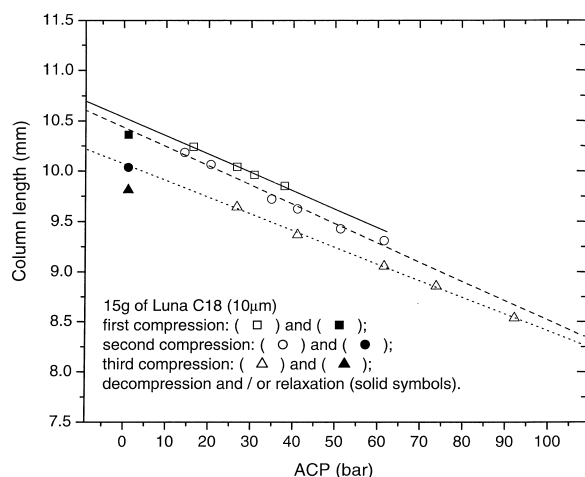


Fig. 5. Compressibility curve for a column packed with 15 g.

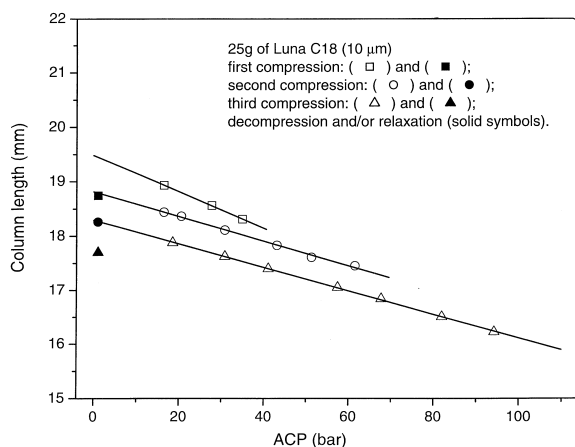


Fig. 6. Compressibility curve for a column packed with 25 g.

pare the compressibility data obtained for two columns packed with fresh stationary phase (ca. 150 g). Column 2 exhibits a compressibility behavior similar to those of the columns packed with 15 and 25 g (Figs. 5 and 6, respectively). However, the extent of the relaxation of its bed upon decompression decreases significantly from the first to the third decompression (see symbols \blacktriangle , \bullet and \blacksquare in Fig. 7). Column 1 was directly compressed up to the maximum stress (ca. 90 bar), without intermediate decompression. Its compression curve is close to the first compression curve of column 2 and would intersect the third compression curve of that column at around 110 bar. The bed lengths of the first column after decompression is close to that of the

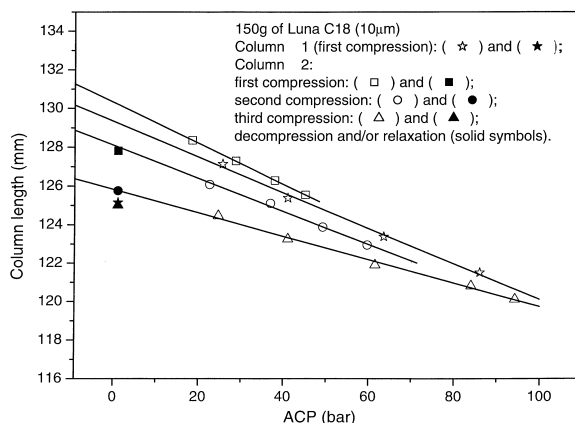


Fig. 7. Compressibility curve for a column packed with 150 g.

second column after the third decompression. This suggests that direct compression at the maximum stress or a series of successive steps of compression followed by decompression produce beds of similar lengths, porosities, and properties (see later, permeability and efficiency). This important result demonstrates that reproducible beds are easily achieved in axially compression systems.

Several other columns were packed in a manner similar to the one described earlier.

Fig. 8 shows the plots of the bed length vs. the axial compression stress for columns packed with 50, 100, 150 (column 1), 200 and 250 g of packing material. For all the columns, the bed length decreases linearly with increasing axial compression stress. The fully consolidated columns expand rapidly when the axial compression stress is released (curves not shown). This result is in agreement with the behavior already reported in previous studies on the consolidation of beds of spherical particles [7–11]. This result is different from the one expected from soil mechanics. Classical consolidation mea-

surements carried out using columns with a low aspect ratio (values of L/D of the order of 0.2 or lower, where L =length and D =diameter) show a lesser influence of the high mechanical stress. The void fraction of these columns $[(1-\epsilon)/\epsilon]$ decreases linearly with increasing logarithm of the compression stress, proportional to the pressure as defined here [23,24].

A consolidated bed of packing material of length L compressed under an axial stress ACP applied to its top (or bottom) shrinks by a length ΔL [23,28]. Its elastic behavior can be characterized by a modulus of elasticity, E :

$$E \text{ (MN m}^{-2}\text{)} = \text{ACP} \frac{L}{\Delta L} \quad (1)$$

Elastic solids have a modulus of elasticity that is independent of their shape or size. Since beds of particles do not fulfill this assumption, we will call apparent modulus the result of applying Eq. (1) to our experimental data. This apparent modulus is an average value, integrating the local modulus over the whole column volume. It must be considered as an empirical parameter. Fig. 9 illustrates the plots of the apparent elasticity modulus, E (MN/m²), of the beds in the consolidation (or compression) mode (\circ symbols) and in the decompression or stress relaxation mode (\triangle symbols). The modulus of elasticity increases considerably with increasing column length because of the radial and axial heterogeneity of the bed. The packing density varies substantially along the column axis due to the wide distribution of the compression stress. The bed is denser close to the piston, where the mechanical stress is highest. The packing density decreases from the piston to the top of the column (Fig. 1). The heterogeneous distribution of the stress, whether axial or radial, creates a stress gradient inside the column. This gradient becomes larger and larger with increasing column length (see later) and is a major limiting factor in the successful packing of very long columns. The variation of the apparent modulus of elasticity with the column length is explained by the friction of the bed of chromatographic columns against their wall, as will be shown later. These results agree with the conclusions of previous studies carried out on similar materials [9,10]. For a homogeneous material, the apparent modulus of elasticity would be constant and independent of the column length.

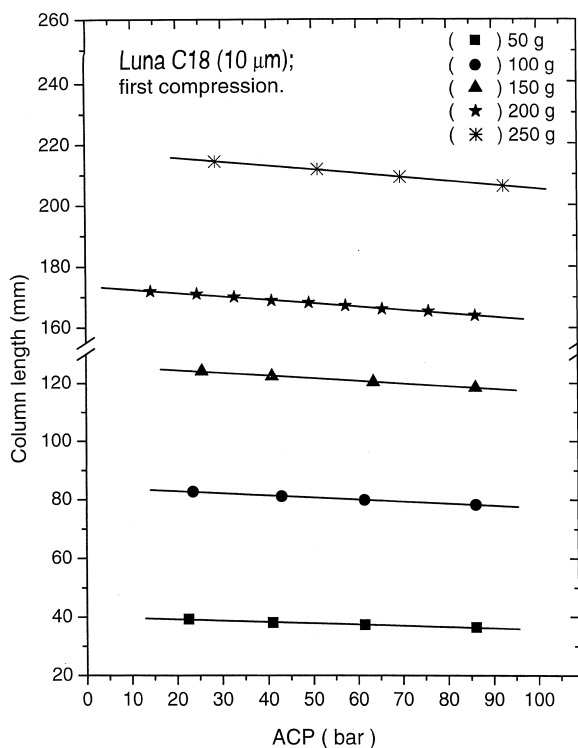


Fig. 8. Compressibility curve for several columns.

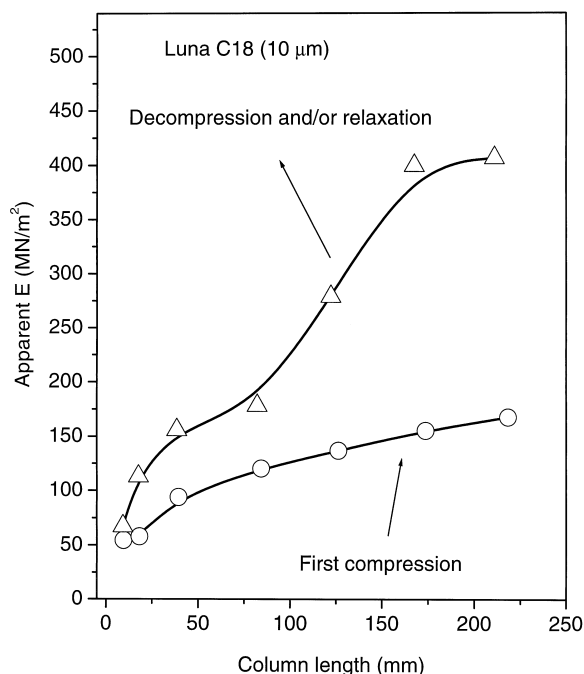


Fig. 9. Plot of the Young or elasticity modulus vs. the bed length at constant compression stress (ca. 40 bar).

The apparent modulus of elasticity in the decompression mode varies substantially with the column length, with an excursion nearly three times larger than that of the apparent modulus of compression, a behavior that was already observed with columns packed with Kromasil C₈ and Zorbax C₁₈ [9,10]. The shortest column (ca. 15 g) exhibits close values for the apparent elasticity modulus in both

modes, E_C and E_R . This small difference could be due to the smaller ratio of the bed length to the column diameter, L/D , for this column and to the higher degree of consolidation achieved for these columns. The difference between the two modulus of elasticity, $(E_R - E_C)$, increases with increasing L/D ratio, due to the wall effect. The compressibility data for the different columns are reported in Table 1. The variation of the apparent Young's modulus in the consolidation mode, E_C , from the first to the third compression, for the column packed with 15 g, is not significant. This demonstrates that a high degree of consolidation is already achieved in the first compression and that the bed behaves elastically when the stress is applied or released (Table 1). For a column packed with 25 g, E_C increases significantly from the first to the second compression and then remains constant when the bed is further compressed.

Meanwhile, E_R , decreases significantly from the first to the second decompression but decreases more strongly from the second to the third decompression. The second column (ca. 150 g) exhibited a moderate increase of E_C from the first to the second compression and a more pronounced one from the second to the third decompression. However, a significant drop of E_R from the first to the second compression and a mere slight change to the third compression were observed (see Table 1). The two columns packed with ca. 150 g (Fig. 7) exhibited similar values of E_C in the first compression, while the value of E_R for the first column was not very different from the one derived from the third compression data for the

Table 1
Compressibility data for some columns

Packing material amount (g)	L (mm) (ACP=86 bar)	1 st compression		2 nd compression		3 rd compression	
		E_C (MN/m ²)	E_R (MN/m ²)	E_C (MN/m ²)	E_R (MN/m ²)	E_C (MN/m ²)	E_R (MN/m ²)
15	8.0	54.5	72.6	51.9	80.9	57.7	67.3
25	16.5	57.8	150.4	83.8	140.7	85.9	113.0
50	36.5	93.9	155.9	na	na	na	na
100	78.3	120.4	178.4	na	na	na	na
150 (column #1)	118.5	137.1	279.3	na	na	na	na
150 (column #2)	119.5	123.4	324.6	149.7	266.6	206.5	240.9
200	164.0	155.8	400.0	na	na	na	na
250	206.2	168.3	407.1	na	na	na	na

E_C and E_R : elasticity module for compression (and/or consolidation) and decompression (and/or relaxation) modes, respectively.

second column. Both columns reached the same degree of consolidation at ca. 100 bar, which indicates that there is not much difference between the degrees of consolidation achieved by either a gradual increase of the mechanical stress, or an abrupt jump to the maximum value, obtained by the direct application of the maximum stress starting from atmospheric pressure (see also permeability).

3.2. Column permeability

The permeability of packed beds is defined as the ratio of the product of the linear flow velocity, the column length, and the mobile phase viscosity to the pressure drop [4]:

$$k_0 = \frac{uL\eta}{\Delta P} \quad (2)$$

It is directly related to the particle size, to their shape, and to the external porosity of the bed, ϵ_e , through the Kozeny–Carman equation (see Ref. [29]):

$$k_0 = \frac{\epsilon_e^3 d_p^2}{\kappa(1 - \epsilon_e)^2} \quad (3)$$

where, κ is a constant, usually taken as 180 for spherical particles [29].

Values of the column permeability were derived from the slope of the plots of the inlet pressure vs. the superficial velocity of the mobile phase (methanol in this study) for flow-rates ranging from 10 to 100 ml/min, using Darcy's law. All the curves (figures not shown) were straight lines. Fig. 10 shows the variation of the column permeability with the axial compression stress during the first consolidation of columns packed with 50, 100, 150, 200 and 250 g of packing material. For all the columns discussed in Fig. 10, the permeability decreases linearly with increasing compression stress. It should be kept in mind that the permeability measured is an average value, integrating the local permeability of the bed in the axial and radial spacial directions. It would be very difficult actually to measure the variation of the permeability along the column axis. Fig. 10 also compares the variation of the permeability with the compression stress for columns packed with 200 g of material during the first and the

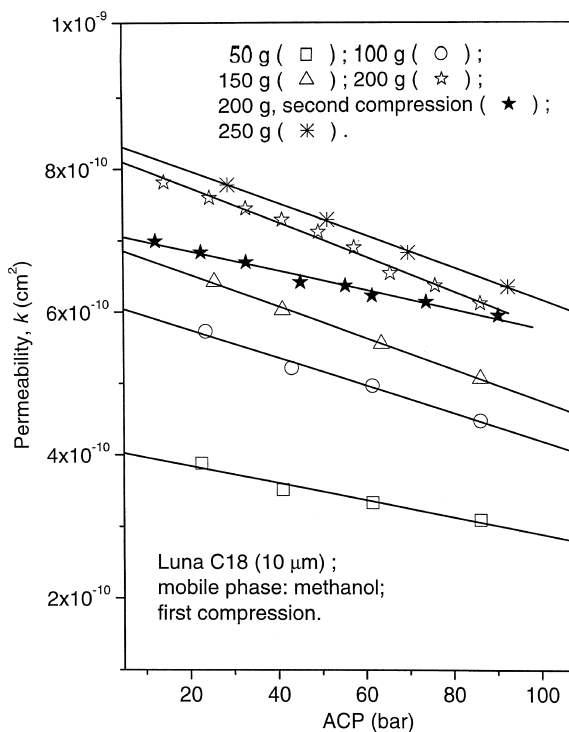


Fig. 10. Plot of permeability versus axial compression stress for some columns.

second compressions. The slopes of the plots of K vs. ACP exhibit a steady decrease from the first to the second compression. The relaxation of the stress or decompression of the bed is accompanied with an expansion of the bed, and an increase of the external porosity resulting in an increase of the column permeability (see the curves for the two columns packed with 200 g of material).

Figs. 11–13 illustrate the influence of the compression stress on the permeability of the columns packed with 15, 25 and 150 g of material, columns whose compression behavior was discussed in the previous section. All three columns exhibit the same behavior. Their permeabilities decrease linearly with increasing axial compression stress and jump back when the stress is released, as do their bed lengths (Figs. 5–7).

However, the slopes of the straight lines decrease from the first to the second compression. The permeability of the relaxed beds, those which are under no applied axial mechanical stress (solid

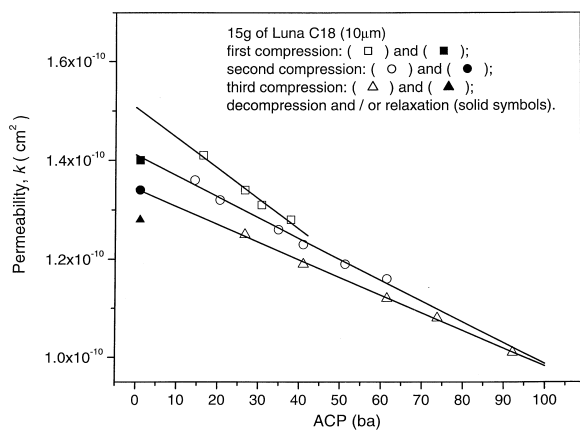


Fig. 11. Plot of permeability versus axial compression stress for a column packed with 15 g.

symbols in Figs. 11–13), decreases significantly between successive compressions, especially for the short columns (those made with 15 and 25 g of packing material). This suggests the possibility that a higher degree of particle breakage takes place in these columns. The curves derived from the measurements carried out on columns 1 and 2 overlap (see Fig. 13). The permeabilities of the relaxed beds of both columns at the end of the last decompression, after compression to the same axial stress (ca. 100 bar) following two different procedures are very similar. This result indicates that reproducible column properties can be well achieved, their compression being robust.

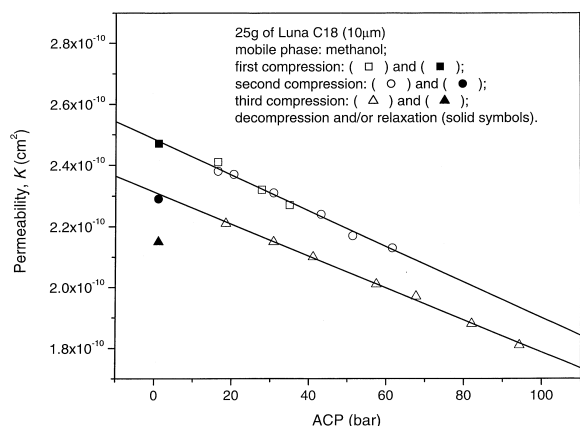


Fig. 12. Plot of permeability versus axial compression stress for a column packed with 25 g.

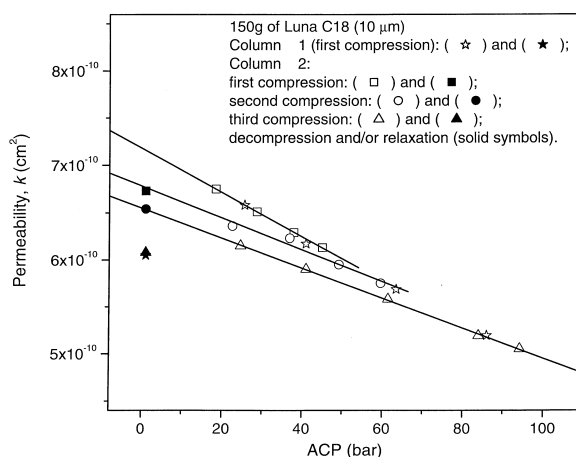


Fig. 13. Plot of permeability versus axial compression stress for a column packed with 150 g.

Plots of the column permeability vs. its length are reported in Fig. 14. The values were derived from the measurements of the dependence of the head pressure on the flow-rate carried out: (a) on the columns compressed up to 86 bar; and (b) on the decompressed beds. Also shown is the length dependence of the values of the permeability extrapolated

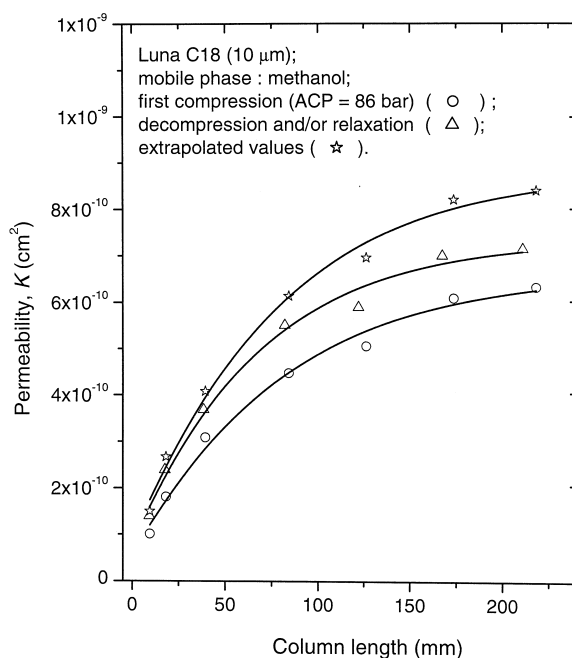


Fig. 14. Permeability vs. bed length.

for a zero compression stress, derived from the linear plots of the permeability versus compression stress (intercept) for each column (see Figs. 10–13). These three estimates of the permeability increase rapidly with increasing length for beds shorter than ca. 75 mm while they increase more slowly for longer beds. This variation is consistent with the heterogeneity of the beds arising from fluctuations of the packing density along and across the column [9,10,27,28]. This behavior was reported in previous studies using similar packing materials [7–11]. The low values of the permeability observed for short columns could be explained by the fact that the axial compression stress employed for all columns was uniformly of 86 bar, which leads to a stronger packing density and possibly to more particle breakage for short columns. Note that the permeability of column packed with ca. 250 g of packing material and has a bed length of ca. 220 mm is 6-fold that of the shortest column (packed with 15 g of material and ca. 10 mm long). Permeability data are summarized in Table 3.

From the values of the permeability plotted in Fig. 14, it is possible to solve Eq. (3) for κ . This requires an accurate estimate for the external porosity, however, because its influence on the permeability is huge. The total porosity of the columns results from the combination of the internal and the external porosities. We assume that the internal porosity remains constant during bed compression, unaffected by the increase of the axial stress. This is legitimate because the particles of silica are rigid and their volume changes little under the stress that they experience in this study. The compression stress affects exclusively the external porosity of the packing bed unless major particle breakage takes place during consolidation under high stress. The internal porosity of the packing material was measured by inverse size exclusion chromatography [30] on an analytical column packed with the same material. Polystyrene samples of narrow molecular mass distributions and known molecular masses were injected on the analytical column using dichloromethane as the mobile phase, at a flow-rate of 1 ml/min. The total porosity of the analytical column was derived from the retention volume of toluene, unretained under the actual experimental conditions. The external porosity was determined from the plot of the logarithm of the molecular mass of the polystyrene

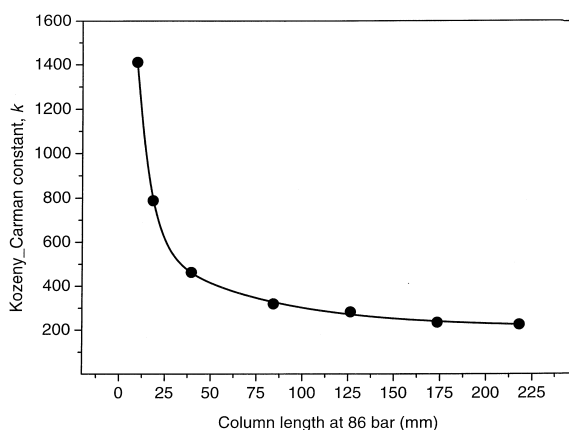


Fig. 15. Kozeny–Carman constant vs. bed length.

vs. its retention volume. A value of the external porosity of ca. 0.38 was derived for the analytical column. Finally, this value was adopted for the calculations, assuming all the columns fully consolidated at stress of ca. 86 bar.

Fig. 15 shows the variation of the Kozeny–Carman constant, κ , vs. the bed length for columns consolidated under a stress of ca. 86 bar (see also Table 2). The constant κ is nearly constant at slightly below 200 for bed lengths longer than 125 mm (a value of ca. 225 is not significantly different from the commonly accepted value of 180) but decreases rapidly for lengths shorter than ca. 100 mm. It decreases nearly 3-fold, from 1410 to 462 when the bed length increases from ca. 9.6 to 39.4 mm (a 4-fold increase). It reaches a value of nearly 1400 for the shortest column, approximately eight times more than the value found for the longest columns and the value that is commonly accepted (ca. 180). This result suggests that an unusually high degree of consolidation of the bed is achieved in

Table 2
Kozeny–Carman constant, k , for different bed lengths at 86 bar

Packing amount (g)	Bed length (mm)	k
15	8.0	1410
25	16.5	788
50	36.5	462
100	78.3	319
150	118.5	282
200	164.0	234
250	206.2	225

short columns and that particle breakage takes place to quite a significant extent during their compression (see earlier), as confirmed by the changes observed in the particle size distribution. This behavior also demonstrates that short columns should be compressed but slightly. The interpretation of this result should also take into account the fact that soil mechanics investigations have shown that the homogeneity of the distribution of the mechanical stress in a bed of sand compressed in a cell of dimensions comparable to those of our column increases with decreasing cell diameter or increasing aspect ratio (D/L) of the bed [31].

3.3. Column efficiency

Fig. 16 shows plots of the reduced plate height vs.

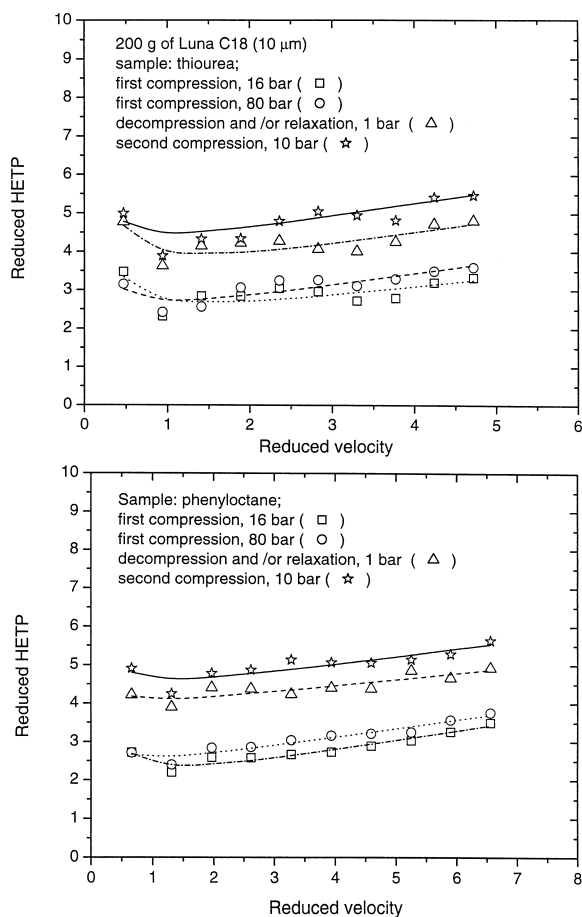


Fig. 16. Plots of reduced HETP vs. reduced velocity.

the reduced velocity of the mobile phase (methanol) for a column packed with 200 g of Luna C₁₈, consolidated under different stresses. A mixture of thiourea and phenyloctane was used as the sample. The volume injected was 0.5 ml. Thiourea is unretained under the actual experimental conditions while phenyloctane has a retention factor nearly equal to unity. Base line separation between the peaks of these two compounds was easily achieved (chromatogram not shown). The efficiencies of both probes were derived from the peak width at half-height and the retention volume of the peak maximum. Injections were performed in a range of linear velocity corresponding to reduced velocities between 0.5 and 5 for thiourea, 0.7 and 7 for phenyloctane. The slightly higher range of reduced linear velocity for phenyloctane is due to a smaller diffusion coefficient of this molecule in methanol (see Fig. 16). The efficiency was corrected for the extra-column contribution to the band variance [10]. The plots in Fig. 16 are typical of those obtained in chromatography. They exhibit a minimum for a reduced velocity between 1 and 3, depending on the curve considered. The reduced HETP varies very slightly in the range of reduced linear velocities considered, due to the fast mass transfer of the two molecular probes used. The experimental data were fitted to the following form of the Van Deemter equation:

$$h = a + \frac{b}{\nu} + c\nu \quad (4)$$

where a , b and c are numerical coefficients. The eddy diffusion term, a , is directly related to the quality of the packing. Poor bed uniformity results in flow channeling and in pathway heterogeneity, spreading the solute band. The parameters b and c correspond to the contributions of axial diffusion and mass transfer resistance, respectively.

We studied the influence of two factors on the column efficiency, the intensity of the axial stress, therefore the degree of consolidation of the bed and the number of consolidation/relaxation steps applied to the bed. Measurements were made at each stress level during several consecutive compressions performed successively. The best performance was obtained when the column was consolidated for the first time, under a compression stress of only ca. 16

bar (symbol \square in Fig. 16). The curves for thiourea and for phenyloctane exhibit both a minimum h equal to nearly 2. After progressive compression and eventual consolidation under ca. 80 bar, the curve has only slightly changed, a change that is barely significant (symbol \circ in Fig. 16). We can conclude that a high axial compression stress does not seem to be required to achieve high column performance and the column efficiency is poorly correlated with the intensity of the axial compression stress. Our best results were obtained with consolidation under a moderate stress.

Then, the compression stress was released and a second compression was undertaken.

The reduced HETP plot obtained for this second compression (symbol \triangle in Fig. 16) is markedly higher than the previous one. The minimum reduced HETP for the column recompressed under a stress of 1 bar is now ca. 4, instead of close to 2 prior to the decompression. This considerable increase of the reduced HETP is difficult to explain by a change in the bed structure since care was taken not to move the bed during the operations of compression and relaxation. However, it seems that, after decompression, the bed has become more heterogeneous. This could have been caused by the displacement of very fine broken particles that could have been trapped inside the frits, creating an uneven flow pattern that could increase the reduced HETP. Nevertheless, good separations can still be obtained with a reduced HETP of ca. 4 but the bed must be handled carefully. A further compression of the bed at 10 bar resulted in a further and significant loss of column efficiency, particularly at high flow velocities, as illustrated in Fig. 16 (symbol \star). This is unfortunate because this velocity range is the most useful range in preparative HPLC.

These results suggest that operating and maintaining axial compression columns under a moderate stress could be beneficial for their performance. Particle breakage is minimized and the column efficiency appears to be higher than under larger stress. Table 3 summarizes the numerical values of the Van Deemter parameters, a , b and c , the reduced HETP at a reduced velocity of ca. 2 and the column permeability, K . Note that, because few measurements of the HETP were made at low flow-rates, the precision on the value of b is very poor. The variations of this permeability are much less important than those of the first Van Deemter coefficients. Comparison of these sets of data confirms that the densest bed is not necessarily the most efficient. As expected, the compression of the bed has little influence of the last two Van Deemter coefficients (Table 3).

3.4. Friction measurements

Friction measurements were carried out on columns packed with different amount of packing material (ca. 15, 25, 50, 100, 150, 200 and 250 g) and consolidated under an axial stress of ca. 40 bar for several hours, after having undergone one or several compression/relaxation cycles with a maximum pressure of ca 90 bar. Detailed description and explanation of the experimental design can be found in previous publications [9,10].

The experimental result is the measured pressure that corresponds to the force $f=P/A$ (with P , pressure applied to the plug and A , cross-section area of the plug) that must be applied on the plug to overcome the shear resistance acting between the bed of packing material and the PTFE plug on the one hand and the column wall on the other hand. The

Table 3
Numerical parameters of the Van Deemter equation (Eq. (4))

ACP (bar)	Thiourea ($D_0 = 1.8 \cdot 10^{-5}$ cm ² /s)				Phenyloctane ($D_0 = 1.3 \cdot 10^{-5}$ cm ² /s)					K 10 ⁻¹⁰ (cm ²)
	a	b	c	h ($u=2$)	a	b	c	h ($u=2$)	k'	
16	1.860	0.640	0.270	2.84	1.570	0.610	0.270	2.69	1.04	7.81
86	1.990	0.410	0.335	3.06	2.110	0.260	0.238	2.76	1.14	6.11
1	2.920	0.750	0.348	4.23	3.720	0.231	0.171	3.95	1.10	7.02
12	3.720	0.422	0.357	4.34	4.050	0.399	0.218	4.52	1.11	6.99

contribution of the PTFE plug must be corrected for. This shear resistance is the integral over the interface area of the shear stress, which depends on the position along the column. The shear resistance of the PTFE plug, f , was measured by carrying out the procedure with an empty column (piston abutting the plug, Fig. 1).

Fig. 17 shows the results obtained with the sole plug (bottom) and with a typical column (top). The solid lines show the record of the inlet pressure of methanol pumped above the plug, the dotted lines, that of the displacement of the piston during the measurement.

Methanol under a set pressure is delivered to the column body, upstream of the PTFE plug, so pressure, hence stress accumulates against the plug. Methanol flows into the column body until the pressure is reached in the column body. If piston does not move, the pressure is increased. This

explains the plateaus observed on the solid lines in Fig. 17. The inlet pressure drops rapidly when the piston begins moving (dotted line). This takes place for pressures of ca. 7 bar (Fig. 17, bottom) and ca. 21 bar (Fig. 17, top).

Then, the pressure stabilizes and varies but slightly during the rest of the experiment while the piston moves at a nearly constant velocity (Fig. 17, dotted lines). Note that the rapid drop of the pressure corresponds exactly to the beginning of the motion of the piston. The uniform sliding of the PTFE plug corresponds to the dynamic frictional resistance which is lower than the static friction between the PTFE plug and the wall, that corresponds to the pressure jump.

Fig. 17 (top) illustrates the results of friction experiments by presenting the record for a column packed with ca. 100 g of Luna C₁₈. The methanol pressure was increased gradually while monitoring the displacement of the piston. A rapid drop of pressure occurred slightly above ca. 20 bar. The difference with the value measured with the PTFE plug gives the shear frictional resistance of the bed alone. At the time the bed begins sliding along the column wall (dotted line), the shear stresses arising from the methanol pressure against the plug overcome the shear stresses that hold the bed against the wall.

The methanol pressure so measured corresponds to the static friction. The methanol pressure plateau reached after ca. 3 min, and accompanied by a steady-state or uniform rate of displacement of the piston corresponds to the dynamic friction. The same behavior was observed for columns packed with different amounts of packing material. Some of the plots of the methanol pressure vs. time recorded are shown in Fig. 18. They are all similar and differ only by the values of the static and dynamic resistances.

Finally, a plot of the methanol pressure versus the bed length is shown in Fig. 19. The pressure increases rapidly with increasing bed length, especially for columns longer than ca. 75 mm. The plot obtained for Luna C₁₈ is very similar to those obtained in previous studies [9,10] for Kromasil C₁₈ and for Zorbax C₁₈. We note, however, that Luna C₁₈ behaves in a way most similar to that of Kromasil but exhibits a much higher frictional resistance for a given column length than Zorbax C₁₈. It is striking

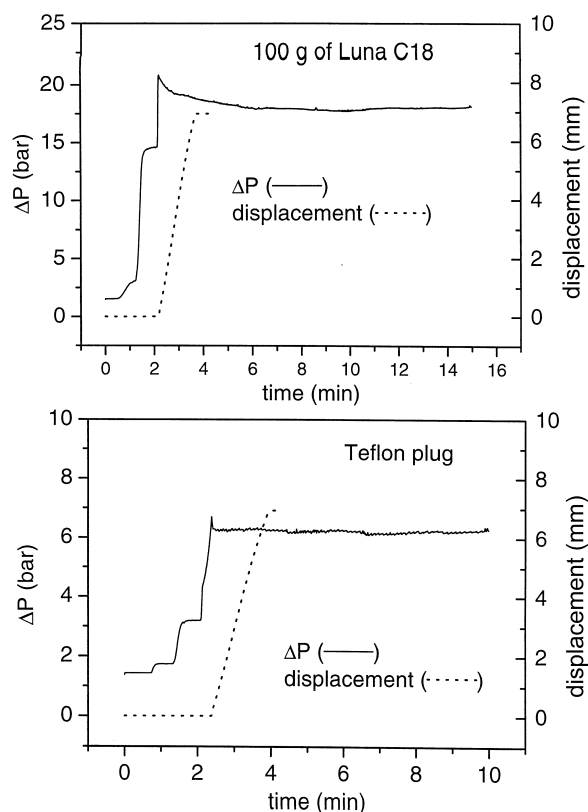


Fig. 17. Friction measurements of a PTFE plug (bottom) and a packed column.

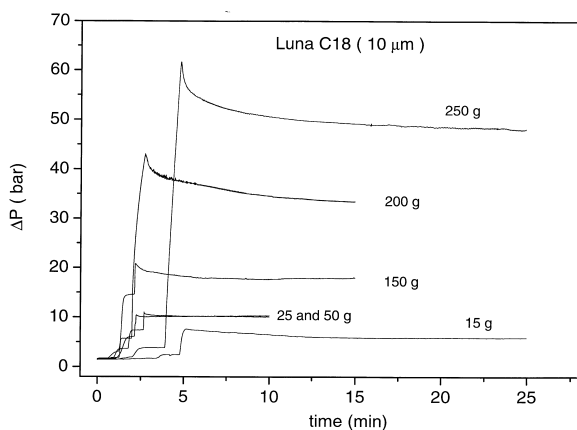


Fig. 18. Effect of the bed length on the friction. Amount of packing material (g) and length (mm) of columns: 1, 15, 8.9; 2, 25, 15.4; 3, 50, 38.0; 4, 100, 81.1; 5, 150, 122.4; 6, 200, 168.8; and 7, 250, 211.4.

that these packing materials, although similar in chemistry, in particle shape and size, and in the average column efficiency obtained with them, exhibit such a different friction behavior. This differ-

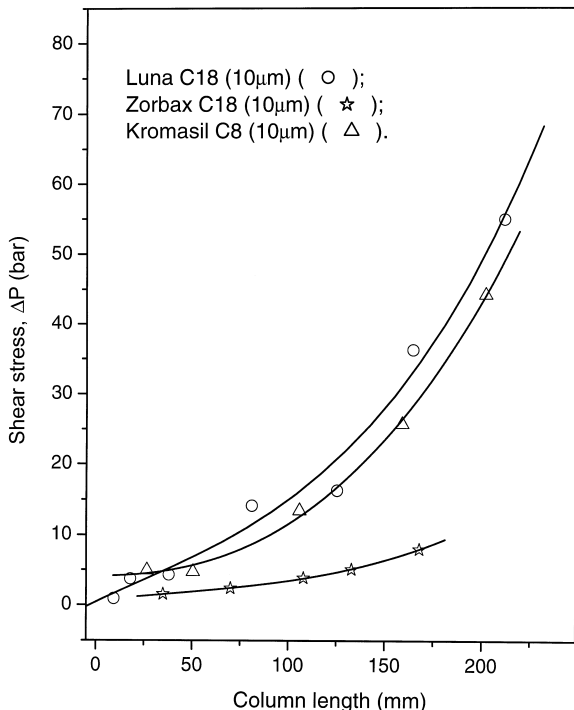


Fig. 19. Plots of the friction shear stress vs. the bed length.

ence could possibly be explained by the less regular particle shape [32] of Zorbax as compared to the other two materials [11] or by a difference in the amounts of fines produced by particle breakage in these materials. This last issue is under investigation.

4. Conclusion

This study confirms the importance of the influence of the wall effect on the performance of packed chromatographic columns. With spherical or nearly spherical particles, consolidation is always fast. The decrease of bed length following the application of an axial stress is nearly instantaneous, with occasional, minor later adjustments. Abrupt stress release also is followed with nearly instantaneous rebound of the length of the consolidated bed. The amplitude of this expansion depends on the intensity of the compression stress but the bed never recovers its length prior to the beginning of the previous compression. After the first compression, the behavior of any bed is elastic but the apparent modulus of elasticity depends on the bed length, underlining the considerable difference between a particulate bed and a true solid. Particle to particle and bed to wall frictions explain these observations.

The results of permeability measurements confirm the heterogeneity of the beds obtained. The permeability depends significantly on the column length. This result is in part explained by the fact that all columns prepared in this study were compressed under the same final stress. It would be useful to repeat similar investigations in which the maximum axial compression stress used to consolidate the beds would be proportional to the column length and in which the properties of columns with lower aspect ratios (lower values of L/D) would be studied in more detail.

These results and, more particularly the importance of the influence of the column length on properties that are usually considered as independent of it may explain why there seems to be a rather small limit to the length of columns that can be efficiently packed by axial compression (Colin, pers. comm., 1998). We note, however, that the column packed with 200 g of Luna C₁₈ exhibited a still most reasonable reduced HETP of ca. 3, at a reduced

velocity of ca. 2 for both thiourea and phenyloctane. As a matter of fact, the most surprising result of this work seems to be, paradoxically, that columns having widely different lengths have nearly the same HETP. This result may be in part explained by the rather low compression pressures at which the best efficiencies are achieved. It is certainly advisable to consolidate and operate preparative columns under moderate pressure and to avoid recompressing them.

Finally, the results of the measurements of the frictional resistance and the length dependence of this resistance that we observed again confirm the critical role of the friction of the bed against the wall in the origin of the wall effect. The critical question, at this stage becomes: will we be able to apply this new knowledge regarding the physical properties of beds of particulate materials and use it to develop better methods of packing columns, leading to far lower reduced column HETP?

Acknowledgements

This work was supported in part by grant DE-FG05-88-ER-13869 of the US Department of Energy and by the cooperative agreement between the University of Tennessee and the Oak Ridge National Laboratory. We acknowledge the loan of the LC.50.VE.500.100 column skid by Prochrom (Cham-pigneulles, France) and the generous gift of Luna C₁₈ packing material by Phenomenex (Torrance, CA, USA). We thank Dr Tivadar Farkas (Phenomenex, Torrance, CA, USA) for fruitful discussions.

References

- [1] G. Guiochon, *J. Chromatogr. A* (2002) in press.
- [2] Y. Shalon, *Am. Lab.*, September (1997) 20N.
- [3] C. Orihuela, R. Fronek, L. Miller, D. Honda, J. Murphy, *J. Chromatogr. A* 827 (1998) 193.
- [4] G. Guiochon, S.G. Shirazi, A.M. Katti, *Fundamentals of Preparative and Nonlinear Chromatography*, Academic Press, Boston, MA, 1994.
- [5] K. Mihlbachler, J. Fricke, T. Yun, A. Seidel-Morgenstern, H. enner Schmidt-Traub, G. Guiochon, *J. Chromatogr. A* 908 (2001) 49.
- [6] T. Zimina, R.M. Smith, J.C. Highfield, P. Myers, B.W. King, *J. Chromatogr. A* 728 (1996) 33.
- [7] M. Sarker, G. Guiochon, *J. Chromatogr. A* 709 (1995) 227.
- [8] J.-H. Koh, G. Guiochon, *J. Chromatogr. A* 796 (1998) 41.
- [9] G. Guiochon, E. Drumm, D. Cherrak, *J. Chromatogr. A* 835 (1999) 41.
- [10] D.E. Cherrak, G. Guiochon, *J. Chromatogr. A* 911 (2001) 147.
- [11] M. Sarker, A.M. Katti, G. Guiochon, *J. Chromatogr. A* 719 (1996) 275.
- [12] J.H. Knox, G.R. Laird, P.A. Raven, *J. Chromatogr.* 122 (1976) 129.
- [13] F.G. Lode, A. Rosenfeld, Q.S. Yuan, T.W. Root, E.N. Lightfoot, *J. Chromatogr. A* 796 (1998) 3.
- [14] A. Brandt, G. Mann, W. Arlt, *J. Chromatogr. A* 769 (1997) 109.
- [15] A. Brandt, G. Mann, W. Arlt, *J. Chromatogr. A* 796 (1998) 223.
- [16] R.A. Shalliker, B.S. Broyles, G. Guiochon, *J. Chromatogr. A* 878 (2000) 153.
- [17] S.G. Harding, H. Baumann, *J. Chromatogr. A* 905 (2001) 19.
- [18] J. Moscariello, G. Purdom, J. Coffman, T.W. Root, E.N. Lightfoot, *J. Chromatogr. A* 908 (2001) 131.
- [19] B. Porsch, *J. Chromatogr. A* 658 (1994) 179.
- [20] A.V. Danilov, L.G. Mustaeva, I.V. Vagenina, M.B. Baru, *J. Chromatogr. A* 732 (1996) 17.
- [21] A.V. Danilov, I.V. Vagenina, L.G. Mustaeva, S.A. Moshnikov, E.Yu. Gorbunova, V.V. Cherskii, M.B. Baru, *J. Chromatogr. A* 773 (1997) 103.
- [22] I.V. Vagenina, E.A. Kozlovsky, L.G. Mustaeva, E.Yu. Gorbunova, M.B. Baru, *J. Chromatogr. A* 840 (1999) 281.
- [23] B.G. Yew, MS Thesis Dissertation, University of Tennessee, Knoxville, TN, USA, 2000.
- [24] B.G. Yew, J. Ureta, E.C. Drumm, G. Guiochon, *AIChE J.*, submitted for publication.
- [25] C.R. Wilke, P. Chang, *AIChE J.* 1 (1955) 264.
- [26] J.J. VanDeemter, F.J. Zuiderweg, A. Klinkenberg, *Chem. Eng. Sci.* 5 (1956) 271.
- [27] G. Guiochon, T. Farkas, H. Guan-Sajonz, J.-H. Koh, M. Sarker, B.J. Stanley, T. Yun, *J. Chromatogr. A* 762 (1997) 83.
- [28] G. Guiochon, M. Sarker, *J. Chromatogr. A* 704 (1995) 247.
- [29] R.B. Bird, W.E. Steward, E.N. Lightfoot, *Transport Phenomena*, Wiley, New York, 1960.
- [30] H. Guan, G. Guiochon, *J. Chromatogr. A* 731 (1996) 27.
- [31] D.W. Taylor, *Fundamentals of Soil Mechanics*, Wiley, New York, 1948.
- [32] J. Krim, *Surf. Sci.* 500 (2002) in press.